Macromolecular Research, Vol. 18, No. 11, pp 1109-1114 (2010)
DOI 10.1007/s13233-010-1107-7
www.springer.com/13233

Luminescent Iron Oxide Nanoparticles Prepared by One-Pot Aphen-Functionalization

Patakamuri Govindaiah, Tae-Joon Park, Yeon Jae Jung, Sun Jong Lee, Du Yeol Ryu, and Jung Hyun Kim*

Department of Chemical and Biomolecular Engineering, Yonsei University, Seoul 120-749, Korea

In Woo Cheong*

Department of Applied Chemistry, Kyungpook National University, Daegu 702-701, Korea

Received May 6, 2010; Revised June 4, 2010; Accepted June 14, 2010

Abstract: 5-Amino-1,10-phenanthroline (Aphen)-functionalized monodisperse luminescent iron oxide nanoparticles were prepared using a one-pot synthetic procedure *via* a thermal decomposition process. Amine functional groups of Aphen as a luminescent source afforded highly stabilized magnetic nanoparticles in polar solvents, resulting in a well-dispersed solution. Transmission electron microscopy (TEM) showed that the size distribution and particle morphology of the iron oxide nanoparticles was improved after anchoring with Aphen. The functionalization of iron oxide nanoparticles with Aphen was examined by UV-vis absorbance and photoluminescence spectroscopy. The Aphen-anchored iron oxide nanoparticles exhibited excellent luminescence properties with an estimated luminescence quantum yield of 0.00354 at room temperature. In addition, these Aphen-anchored iron oxide nanoparticles were characterized by vibrating sample magnetometry (VSM) to reveal the magnetic properties. The Aphen-anchored iron oxide nanoparticles exhibited both luminescence and magnetic properties.

Keywords: luminescent, iron oxide, inorganic-organic hybrid, aphen-functionalized, nanoparticles.

Introduction

The application of magnetic nanoparticles has become an enabling technology and has quickly attracted the interest of scientists studying magnetic fields,[1] catalysis,[2,3] biomedicine,[4,5] magnetic resonance imaging,[6] data storage,[7,8] and environmental remediation.[9-13] In particular, the synthesis of multifunctional magnetic nanoparticles having both optical and magnetic properties are becoming more important because of their multiple utilities such as site-selective binding,[14,15] biosensing,[16] and bioseparation.[17] Fe,[18,19] Co,[20] γ-Fe_2O_3,[21] and Fe_3O_4[22,23] are the most interesting magnetic nanoparticles, and thus have been synthesized by using various synthetic methods including co-precipitation,[24] thermal decomposition,[25,26] arc-plasma assisted CVD,[27] and hydrothermal reduction.[28]

The ability to obtain multifunctional properties in the single nano-object has developed extensively in recent years. Multicomponent hybrid nanostructures were prepared by integrating two or more nanoparticle components into a single nano-system such as, CdSe-Fe_3O_4,[29] Ag-Fe_3O_4,[30,31] Au-FePt,[32] and the magnetic nanoparticle surface was also functionalized by organic chromophore ligands.[33,34] In spite of the ongoing success of the synthesis of multifunctional nanoparticles, the interaction between magnetic nanoparticles and luminescent functional ligands have rarely been focused on.[35,36] To date, two major approaches have been developed to modify the surface of nanoparticles using organic ligands.[37,38] The first approach is based on coordinate bonding. Functional groups like, thiols, carboxylic acids, and dopamines, were used directly to link hydrophilic groups onto the surface of hydrophobic nanoparticles by replacing original hydrophobic ligands.[39-41] The second approach uses van der Waals interactions, through which the hydrophobic tails of amphiphilic ligands interact with, but do not replace, the hydrophobic ligands on the surface of nanoparticles, thus leading to the formation of nanoparticle micelles.[42] While these approaches provide valuable information on the surface modification of nanoparticles using organic ligands, the drawback is the weak interactions between the ligand and metal particle. Hence the current work uniquely addresses this problem by an alternative approach to functionalize organic chromophores such as Aphen onto the surface of Fe_3O_4 nanoparticles via one-pot synthesis.

Aphen is one of the widely used chelating ligands in coordination chemistry due to its high affinity towards various

*Corresponding Authors. E-mails: jayhkim@yonsei.ac.kr or inwoo@knu.ac.kr

cations and metal complexes.[43,44] The magnetic core normally quenches the fluorescence of functionalized chromophore and this problem can be resolved by covalent bonding of chromophore to the magnetic nanoparticle via an appropriate spacer.[33,34] Aphen is an active functional ligand which can provide surface stability by coordination and it also provides luminescence properties to the metal particle. It can coordinate with metal ions through a nitrogen atom,[45] and provide reactive -NH_2 functional groups for further covalent attachment. Aphen-functionalized Fe_3O_4 nanoparticles can retain the magnetic and optical properties of each component and permit potential applications as optical reporters and magnetic handles for bioassay. Functionalization of Aphen onto gold particles has been extensively studied in our previous work[46] and, to our knowledge, anchoring Aphen onto iron oxide nanoparticles has not been studied. We turned our attention to Aphen as a functional ligand due to its high affinity for metallic surfaces.[47-51]

In this article, we report a new type of nanocomposite materials based on magnetic nanoparticles and Aphen, with direct and strong interactions between organic ligand and metal nanoparticles. In the one-pot thermal decomposition process, $Fe(acac)_3$ was used as a single iron source. Oleylamine (OAm) as both a surface stabilizer and a reducing agent and Aphen were chosen as a luminescent source to obtain surface coordinated luminescent multifunctional magnetic nanoparticles.

Experimental

Materials and Reagents. 5-Amino-1,10-phenanthroline (Aphen), Oleylamine (OAm), Iron(III) acetylacetonate ($Fe(acac)_3$), 1,2-dodecandiol and benzyl ether were purchased from Aldrich, USA. Ethanol and hexane were purchased from Duksan Chemical, Korea. All reagents were used as received without further purification.

Preparation of Fe_3O_4-OAm Nanoparticles. OAm-functionalized magnetic nanoparticles were prepared in a thermal decomposition process. In a typical preparation, 0.706 g of $Fe(acac)_3$, 2.023 g of 1,2-dodecanediol, 1.605 g OAm, and 80 mL benzyl ether were mixed in a round bottom flask and purged with nitrogen to remove oxygen. The mixture was heated to reflux for 30 min and then cooled to room temperature. Addition of ethanol to the reaction solution resulted in a dark-brown precipitate which was washed with ethanol for several times by magnetic separation and then dried under vacuum at room temperature.

Preparation of Fe_3O_4-OAm-Aphen Nanoparticles. Magnetic nanoparticles anchored with mixed ligands were prepared in a similar fashion to the above procedure. In a typical preparation, 0.706 g of $Fe(acac)_3$, 2.023 g of 1,2-dodecanediol, 1.605 g of OAm, 0.098 g Aphen, and 80 mL of benzylether were mixed in a round bottom flask and purged with nitrogen to remove oxygen. The mixture was heated to reflux for 30 min and then cooled to room temperature. Addition of hexane to the reaction solution resulted in a dark-brown precipitate which was washed with a hexane/ethanol (95/5, v/v) solution several times by magnetic separation and then dried under vacuum at room temperature.

Quantum Yield Mesurements. PL quantum yields of Aphen-functionalized magnetic nanoparticles in ethanol (ca. 0.8196×10^{-5} M) was measured by comparing with quinine sulfate (ca. 0.8196×10^{-5} M) in 0.10 M H_2SO_4 as standard according to following equation:

$$\Phi_{unk} = \Phi_{std}(I_{unk}/I_{std})(A_{std}/A_{unk})(\eta_{unk}/\eta_{std})^2$$

Φ corresponds to the quantum yields, I to the integrated PL emission intensity excited at the maximum wavelength of UV absorbance, A to the absorbance at the excitation wavelength at the same concentration, and η to the refractive index of the solvents used. Subscripts *unk* and *std* correspond to the unknown and the standard, respectively.

Characterization. Infrared spectra were recorded on FT IR (Tensor 27, Bruker, Germany) as potassium bromide pellets. All samples were scanned between 400 and 4500 cm^{-1} as transmittance spectra. The WAXD experiments were performed on an X-ray diffractometer (DMAX 2500, Rigaku, Japan) equipped with a copper target and a diffracted beam monochromator (Cu Kα radiation with λ=1.5406 Å) with 2θ scan range of 5~80° at room temperature. Powdered samples were pressed on a glass plate sample holder. The morphology of nanoparticles was observed by using TEM (JSM 100CXII, JEOL, Japan). A High-resolution TEM (HR-TEM) (JEM-3010, JEOL, Japan) was used to capture high resolution images. The absorption spectra were obtained with a UV-vis spectrophotometer (UV-1601PC, Shimadzu, Japan). Photoluminescence (PL) spectra were recorded with a spectrofluorophotometer (RF-5301PC, Shimadzu, Japan). Excitation was incident at an angle of 0° onto the front face of the sample, and the emission was recorded in reflection at an angle of 90° with respect to the surface normal. The thermal properties of the samples were analyzed by TGA (Q50, TA instruments); TGA was used to determine the organic ligand quantity. The samples were heated under flowing nitrogen atmosphere from 50 to 800 °C at a heating rate of 10 °C/min and the weight loss was recorded. The magnetization measurements were performed at room temperature using a vibrating sample magnetometer (VSM) (450-10, LakeShore). The saturation magnetization values were normalized to the mass of nanoparticles to yield the specific magnetization, M (emu/g).

Results and Discussion

Scheme I illustrates the synthetic pathway for making Aphen-functionalized iron oxide nanoparticles. As shown in Scheme I, Aphen was anchored onto iron oxide nanoparticles by coordination. Aphen coordinates with iron

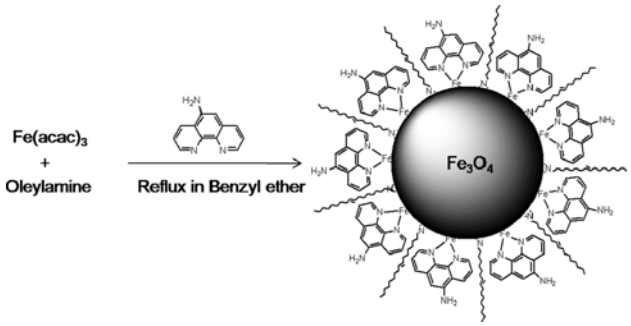

Scheme I. A schematic for the synthesis of Aphen-functionalized iron oxide nanoparticles.

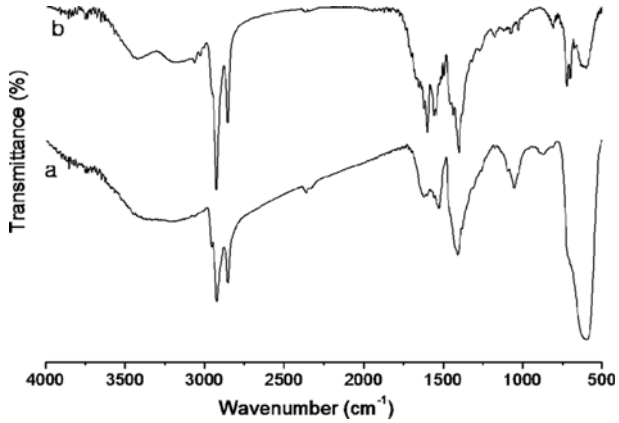

Figure 1. FTIR spectra of functionalized magnetic nanoparticles (a) Fe_3O_4-OAm and (b) Fe_3O_4-OAm-Aphen.

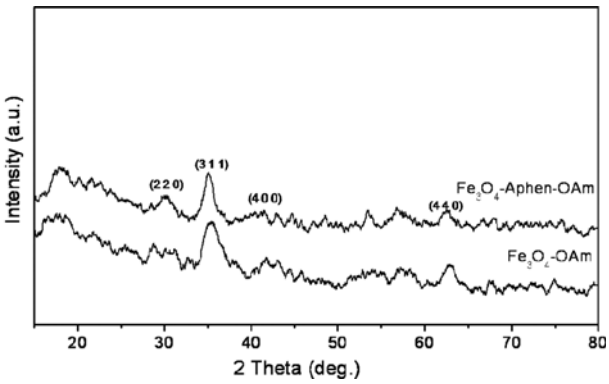

Figure 2. XRD spectra of functionalized magnetic nanoparticles.

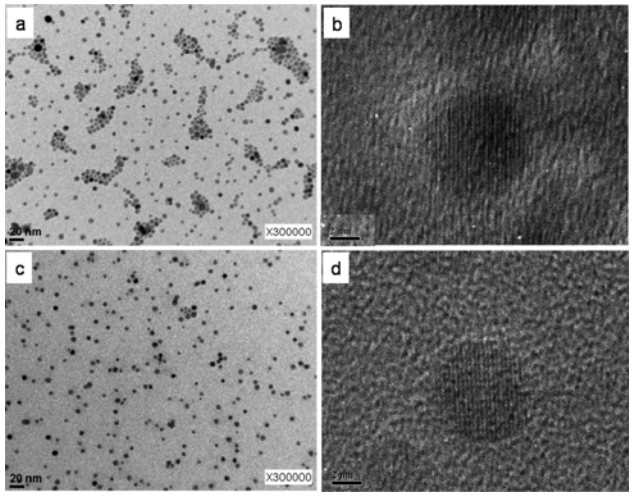

Figure 3. TEM images of Fe_3O_4 nanoparticles prepared by one-pot synthesis: (a) Fe_3O_4-OAm and (c) Fe_3O_4-OAm-Aphen; HR-TEM images of (b) Fe_3O_4-OAm and (d) Fe_3O_4-OAm-Aphen.

oxide nanoparticles via nitrogen atom. OAm provides surface stability to iron oxide particles by anchoring onto the surface.

The FTIR spectra of the two samples, Fe_3O_4-OAm, and Fe_3O_4-OAm-Aphen nanoparticles, are shown in Figure 1. The presence of surface-functionalized organic ligands can be confirmed in the FTIR spectra. The band at 600 cm^{-1} was assigned to the vibration of the Fe-O bond of the iron oxide core. A band at 1608 cm^{-1} corresponds to N-H bending, 808 cm^{-1} corresponds to out of plane N-H bending and the bands at around 3420 cm^{-1}, 3175 cm^{-1} corresponds to the N-H stretching vibrations. In the spectrum of Fe_3O_4-OAm-Aphen nanoparticles, the bands at around 3065 cm^{-1} are assigned to aromatic C-H stretching and the bands at around 2844-2925 cm^{-1} are assigned to aliphatic C-H stretching.

X-ray diffraction (XRD) was used to record the crystal information of iron oxide nanoparticles. Figure 2 shows the XRD patterns of iron oxide nanoparticles covered with OAm and mixed ligands. Functionalized magnetic nanoparticles could be indexed to the (2 2 0), (3 1 1), (4 0 0), and (4 4 0) planes of magnetite (Fe_3O_4) nanoparticles.[33] All diffraction peak positions match well with standard Fe_3O_4 peak positions.

Figure 3 presents representative transmission electron microscope (TEM) images of the Fe_3O_4 nanoparticles with various ligand-functionalized surfaces. The morphology and solubility behavior of the magnetic nanoparticles can be controlled simply by selecting surface-functionalized ligands. Both Fe_3O_4-OAm and Fe_3O_4-OAm-Aphen nanoparticles showed spherical morphology. In addition, Fe_3O_4-OAm-Aphen nanoparticles showed a narrow particle size distribution with sizes ranging from 5 to 8 nm, as compared with the Fe_3O_4-OAm nanoparticles. In this work, the mixed ligands were used in order to enhance the stability of the nanoparticles. Enhancement in the particle stability may be due to the balanced structure of surface-functionalized ligands. The lattice fringe in HR-TEM images corresponds to a group of atomic planes within a single crystal of Fe_3O_4 nanoparticle.

To examine the relative quantity of organic ligands functionalized onto the surface of Fe_3O_4 nanoparticles, TGA measurements were performed and the results are shown in Figure 4. The Fe_3O_4-OAm showed a weight loss of 10 wt% at 700 °C. Fe_3O_4-OAm-Aphen nanoparticles showed weight loss of about 52 wt% at 700 °C. These results indicate that 52 wt% of the organic ligands were anchored onto 48 wt% iron oxide nanoparticles surface. Figure 5 shows the dispersion

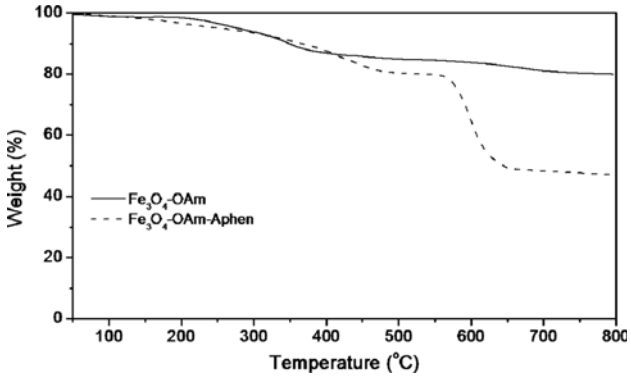

Figure 4. TGA thermogram of functionalized magnetic nanoparticles.

Figure 5. Dispersion behavior of Fe_3O_4-OAm-Aphen nanoparticles in various solvents.

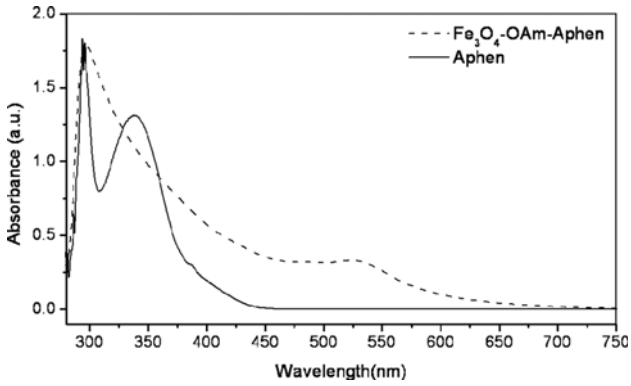

Figure 6. UV-visible absorption spectra of Aphen-functionalized iron oxide nanoparticles and Apehn/ethanol solution.

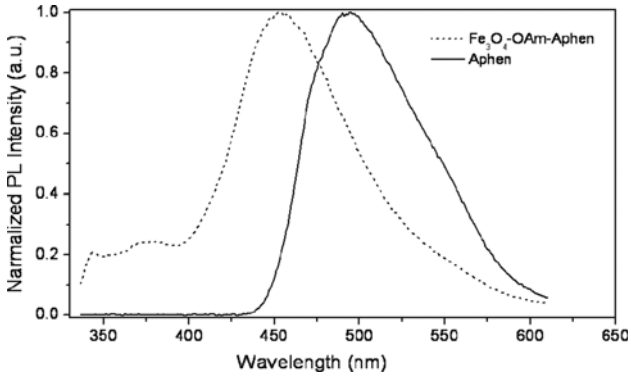

Figure 7. Normalized PL spectra of Aphen and Aphen-functionalized iron oxide nanoparticles.

behavior of Aphen-functionalized iron oxide nanoparticles in various solvents. The dark brown powder of Aphen-functionalized magnetic nanoparticles was proven to exhibit good dispersibility in polar solvents (i.e., alcohols) to form a stable ferrofluid. Since the magnetic nanoparticles that OAm only covered are capable of being dispersed in non-polar solvents and the magnetic particle surface was modified by Aphen functionalization, these magnetic nanoparticles were well dispersed in ethanol and chloroform but not in hexane. The dispersion behavior of magnetic nanoparticles in the various solvents was shown to be strongly dependent on the surface-anchored ligands.

Figure 6 compares the UV-vis absorption spectra of Aphen-functionalized iron oxide nanoparticles. The ethanolic solution of Aphen possesses well-defined absorption bands in the UV-region (296 and 330 nm) corresponding to the π-π^* intra-ligand transition from the Aphen chromophore. After the functionalization, a single absorption band indicating the intra-ligand transition was observed at 300 nm. In addition, a broad band at 525 nm was observed, which can be attributed to the admixture of the metal-to-ligand charge transfer (MLCT) band of the Aphen and iron oxide. These results confirmed that the Aphen-functionalization was achieved successfully onto the iron oxide nanoparticles.

The fluorescence emission spectra of the Aphen-functionalized magnetic nanoparticles and pure Aphen in ethanol solution with excitation wavelength at 310 nm were compared in Figure 7. Aphen-functionalized magnetic nanoparticles showed an emission peak at 448 nm, which is shifted significantly to the blue region compared with the emission spectrum of pure Aphen (λ_{em}=494 nm). This blue shift indicates that Aphen is anchored onto the surface of the iron oxide nanoparticles. Luminescence quantum yields (Φ) of Aphen-functionalized iron oxide nanoparticles in ethanol were estimated by comparing with a known quantum yield of quinine sulfate.[52] The quantum yields of Fe_3O_4-OAm-Aphen were estimated to be 0.00354. Figure 8 shows digital pictures of Fe_3O_4-OAm-Aphen in ethanol before and after UV irradiation. After UV irradiation, the red color solution emitted blue light at 312 nm. These results imply that the fluorescence of surface anchored-chromophore is not quenched by superparamagnetic core.

The magnetic moment of as-synthesized iron oxide nanoparticles was measured with a vibrating sample magnetometer as a function of applied magnetic field at 10 K. Both

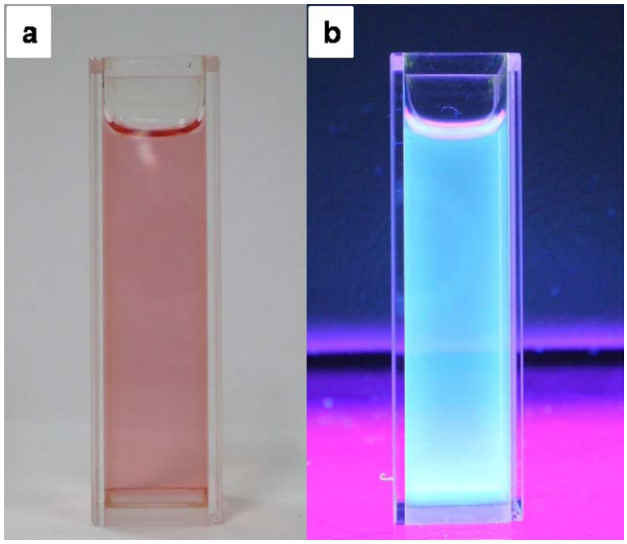

Figure 8. Digital images of ethanol dispersed Fe_3O_4-OAm-Aphen nanoparticles (a) before and (b) after UV irradiation at 312 nm.

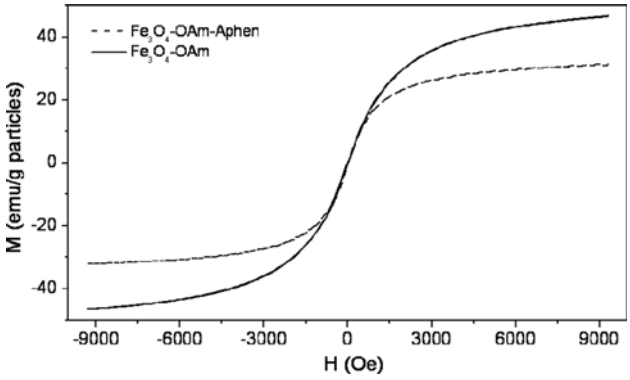

Figure 9. Magnetic hysteresis loops of iron oxide nanoparticles synthesized by one-pot synthesis.

Fe_3O_4-OAm and Fe_3O_4-OAm-Aphen nanoparticles exhibit the superparamagnetic characteristics. As seen in Figure 9, the saturation magnetizations of Fe_3O_4-OAm and Fe_3O_4-OAm-Aphen were 46 and 31 emu/g, respectively. The difference in the saturation magnetization of the synthesized nanoparticles would be mainly attributed to the difference in the surface-anchored functional groups. The saturation magnetization of Fe_3O_4-OAm-Aphen nanoparticles was lower than those of OAm-functionalized iron oxide nanoparticles, which was caused by the surface spin effects.[53]

Conclusions

In conclusion, we have synthesized Aphen-functionalized luminescent magnetic nanoparticles by a simple and one-pot reaction. In this work, OAm acted as a surface stabilizer as well as a reducing agent. Surface-anchored Aphen provided luminescent properties to the iron oxide nanoparticles. Particle morphology and size distribution were dependent on the nature of surface-anchored ligands. Fe_3O_4-OAm-Aphen nanoparticles showed good luminescent properties with enhanced quantum yield. In addition, these luminescent iron oxide nanoparticles exhibit superparamagnetic characteristics. Therefore, these nanoparticles, with luminescence, magnetic properties, good dispersibility, and further functionalization capability, can be effectively utilized in practical applications of biomedicine, labeling, detection, and bioseparation.

Acknowledgements. This work was financially supported by the Research Foundation (NRF) grant funded by the Korea government (MOST) through the Active Polymer Center for Pattern Integration (Nos. R11-2007-050-00000-0) and grant from the Industrial Technology Development program (K0006005) of the Ministry of Knowledge Economy (MKE) of Korea. This research was supported by Nano R&D program through the National Research Foundation (NRF) of Korea funded by the Ministry of Education, Science and Technology (2009-0083233). This work was supported by Mid-career Research and Business Development Program through NRF grant funded by the MEST (No. 2007-0052622). This work was also supported by the Seoul Research and Business Development Program (10816).

References

(1) S. Chikazumi, S. Taketomi, M. Ukita, M. Mizukami, H. Miyajima, M. Setogawa, and Y. Kurihara, *J. Magn. Magn. Mater.*, **65**, 245 (1987).
(2) A.-H. Lu, W. Schmidt, N. Matoussevitch, H. Bonnermann, B. Spliethoff, B. Tesche, E. Bill, W. Kiefer, and F. Schuth, *Angew. Chem. Int. Ed.*, **43**, 4303 (2004).
(3) S. C. Tsang, V. Caps, I. Paraskavas, D. Chadwick, and D. Thompsett, *Angew. Chem. Int. Ed.*, **43**, 5643 (2004).
(4) A. K. Gupta and M. Gupta, *Biomaterials*, **26**, 3995 (2005).
(5) S. M. Kang, I. S. Choi, K. B. Lee, and Y. S. Kim, *Macromol. Res.*, **17**, 259 (2009).
(6) Z. Li, L. Wei, M. Y. Gao, and H. Lei, *Adv. Mater.*, **17**, 1001 (2005).
(7) T. Hyeon, *Chem. Commun.*, 927 (2003).
(8) S. Sun, C. B. Murray, D. Weller, L. Folks, and A. Moser, *Science*, **287**, 1989 (2000).
(9) M. Takafuji, S. Ide, H. Ihara, and Z. Xu, *Chem. Mater.*, **16**, 1977 (2004).
(10) A.-H. Lu, E. L. Salabas, and F. Schuth, *Angew. Chem. Int. Ed.*, **46**, 1222 (2007).
(11) A. Ito, M. Shinkai, H. Honda, and T. Kobayashi, *J. Biosci. Bioeng.*, **100**, 1 (2005).
(12) Q. A. Pankhurst, J. Connolly, S. K. Jones, and J. Dobson, *J. Phys. D: Appl. Phys.*, **36**, R167 (2003).
(13) C. C. Berry and A. S. G. Curtis, *J. Phys. D: Appl. Phys.*, **36**, R198 (2003).
(14) T. Andrew Taton, *Nature Materials*, **2**, 73 (2003).
(15) H. W. Gu, P. L. Ho. K. W. T. Tsang, L. Wang, and B. Xu, *J. Am. Chem. Soc.*, **125**, 15702 (2003).

(16) P. I. Nikitin, P. M. Vetoshko, and T. I. Ksenevich, *J. Magn. Magn. Mater.,* **311**, 445 (2007).
(17) Y. Zhang, G. M. Zeng, L. Tang, D. L. Huang, X. Y. Jiang, and Y. N. Chen, *Biosens. Bioelectron.,* **22**, 2121 (2007).
(18) S.-J. Park, *J. Am. Chem. Soc.,* **112**, 8581 (2000).
(19) S. Peng, C. Wang, J. Xia, and S. Sun, *J. Am. Chem. Soc.*, **128**, 10676 (2006).
(20) S. Sun and C. B. Murray, *J. Appl. Phys.,* **85**, 4325 (1999).
(21) J. Rockenberger, E. C. Scher, and A. P. Alivisatos, *J. Am. Chem. Soc.,* **121**, 11595 (1999).
(22) S. Sun, H. Zeng, D. B. Robinson, S. Raoux, P. M. Rice, S. X. Wang, and G. Li, *J. Am. Chem. Soc.,* **126**, 273 (2004).
(23) H. Ahmad, M. Abdur Rahman, M. A. Jalil Miah, and K. Tauer, *Macromol. Res.*, **16**, 637 (2008).
(24) C. M. Lee, H. J. Jeong, E. M. Kim, S. J. Cheong, E. H. Park, D. W. Kim, S. T. Lim, and M. H. Sohn, *Macromol. Res.,* **17**, 133 (2009).
(25) C. Murray, D. J. Norris, and M. G. Bawendi, *J. Am. Chem. Soc.,* **115**, 8706 (1993).
(26) Y. H. Kim, J. H. Choi, and S. H. Kim, *Macromol. Res.*, **17**, 5 (2009).
(27) Z. Li, C. Hu, C. Yu, and J. Qiu, *J. Nanosci. Nanotechnol.,* **9**, 7473 (2009).
(28) H. Deng, X. Li, Q. Peng, X. Wang, J. Chen, and Y. Li, *Angew. Chem. Int. Ed.,* **44**, 2782 (2005).
(29) S. T. Selvan, P. K. Patra, C. Y. Ang, and J. Y. Ying, *Angew. Chem. Int. Ed.*, **46**, 2448 (2007).
(30) H. Zeng and S. Sun, *Adv. Funct. Mater.,* **18**, 391 (2008).
(31) H. W. Gu, Z. M. Yang, J. H. Gao, C. K. Chang, and B. Xu, *J. Am. Chem. Soc.,* **127**, 34 (2005).
(32) Z.-S. Choi, Y.-W. Jun, S.-I. Yeon, H. C. Kim, J.-S. Shin, and J. Cheon, *J. Am. Chem. Soc.,* **128**, 15982 (2006).
(33) H. Gu, K. Xu, Z. Yang, C. K. Chang, and B. Xu, *Chem. Commun.,* 4270 (2005).
(34) S. A. Corr, A. O' Byrne, Y. K. Gun'ko, S. Ghosh, D. F. Brougham, S. Mitchell, Y. Volkov, and A. Prina-Mello, *Chem. Commun.,* 4474 (2006).
(35) C.-W. Lai, Y. H. Wang, C.-H. Lai, M.-J. Yang, C.-Y. Chen, P.-T. Chou, C.-S. Chan, Y. Chi, Y.-C. Chen, and J.-K. Hsiao, *Small,* **4**, 218 (2008).
(36) J. Choi, J. C. Kim, Y. B. Lee, I. S. Kim, Y. K. Park, and N. H. Hur, *Chem. Commun.,* 1644 (2007).
(37) A. P. Alivisatos, *Nat. Biotechnol.,* **22**, 47 (2004).
(38) H. Wu, H. Zhu, J. Zhuang, S. Yang, C. Liu, and Y. C. Cao, *Angew. Chem. Int. Ed.,* **47**, 3730 (2008).
(39) J. Tian, Y. K. Feng, and Y. S. Xu, *Macromol. Res.*, **14**, 209 (2006).
(40) R. D. Palma, S. Peeters, M. J. Van Bael, H. Van den Rul, K. Bonroy, W. Laureyn, J. Mullens, G. Borghs, and G. Maes, *Chem. Mater.,* **19**, 1821 (2007).
(41) H. G. Bagaria, E. T. Ada, M. Shamsuzzoha, D. E. Nikles, and D. T. Johnson, *Langmuir,* **22**, 7732 (2006).
(42) G. M. Kloster, C. M. Taylor, and S. P. Watton, *Inorg. Chem.,* **38**, 395 (1999).
(43) J. Gao, C. Lu, X. Lu, and Y. Du, *J. Mater. Chem.*, **17**, 4591 (2007).
(44) Q. M. Wang and B. Yen, *J. Photochem. Photobiol. A*, **178**, 70 (2006).
(45) L. G. Bachas, L. Cullen, R. S. Huthins, and L. Scott, *J. Chem. Soc., Dalton Trans.*, 1571 (1997).
(46) P. Govindaiah, J. M. Lee, Y. J. Jung, S. J. Lee, and J. H. Kim, *J. Mater. Chem.,* **19**, 3529 (2009).
(47) U. R. Pillai and E. Sahle-Demessie, *J. Mol. Catal. A: Chem.,* **222**, 153 (2004).
(48) J. Huang, T. Jiang, B. Han, H. Gao, Y. Chang, G. Zhao, and W. Wu, *Chem. Commun.,* 1654 (2003).
(49) N. Toshima, Y. Shiraishi, T. Teranishi, M. Miyaki, T. Tominaga, H. Watanabe, W. Brijoux, H. Bonnemann, and G. Schmid, *Appl. Organometal. Chem.,* **15**, 178 (2001).
(50) M. Muniz-Miranda, *J. Phys. Chem. A,* **104**, 7803 (2000).
(51) C. R. Mayer, E. Dumas, and F. Scheresse, *J. Colloid Interface Sci.*, **328**, 452 (2008).
(52) Z.-K. Chen, W. Huang, L.-H. Wang, E.-T. Kang, B. J. Chen, C. S. Lee, and S. T. Lee, *Macromolecules*, **33**, 9015 (2000).
(53) C. R. Vestal and Z. J. Zhang, *J. Am. Chem. Soc.,* **125**, 9828 (2003).